Particle-Filtering-Based Discharge Time Prognosis for Lithium-Ion Batteries With a Statistical Characterization of Use Profiles

Daniel A. Pola, Hugo F. Navarrete, Marcos E. Orchard, *Member, IEEE,*
Ricardo S. Rabié, Matías A. Cerda, Benjamín E. Olivares, Jorge F. Silva, *Member, IEEE,*
Pablo A. Espinoza, and Aramis Pérez

Abstract—We present the implementation of a particle-filtering-based prognostic framework that utilizes statistical characterization of use profiles to (i) estimate the state-of-charge (SOC), and (ii) predict the discharge time of energy storage devices (lithium-ion batteries). The proposed approach uses a novel empirical state-space model, inspired by battery phenomenology, and particle-filtering algorithms to estimate SOC and other unknown model parameters in real-time. The adaptation mechanism used during the filtering stage improves the convergence of the state estimate, and provides adequate initial conditions for the prognosis stage. SOC prognosis is implemented using a particle-filtering-based framework that considers a statistical characterization of uncertainty for future discharge profiles based on maximum likelihood estimates of transition probabilities for a two-state Markov chain. All algorithms have been trained and validated using experimental data acquired from one Li-Ion 26650 and two Li-Ion 18650 cells, and considering different operating conditions.

Index Terms—Lithium-ion battery, Markov chain, particle filtering, state-of-charge prognosis.

ACRONYMS AND ABBREVIATIONS

EIS	Electrochemical Impedance Spectroscopy
EOD	End-of-Discharge
ESD	Energy Storage Device
EWMA	Exponentially Weighted Moving Average
FUDS	Federal Urban Driving Schedule
JITP	Just-In-Time Point
MC	Markov Chain
OCV	Open-Circuit Voltage
PF	Particle Filters
PDF	Probability Density Function
SMC	Sequential Monte Carlo
SOC	State-of-Charge

NOTATION

$w_k^{(i)}$	Weight associated with the ith particle at time k
$x_{0:k}^{(i)}$	Realization of the state vector trajectory, associated with the ith particle at time k
φ^k	π_k-integrable function
$\pi_k(x_{0:k})$	True state vector probability density function
$y_{1:k}$	Measurements collected up to time k
$p(x_{0:k}|y_{1:k})$	Posterior density function of the state vector, conditional to noisy measurements
$q(\tilde{x}_{0:k}|x_{0:k-1})$	Importance sampling distribution for state vector transition in time
$K(\cdot)$	Kernel density function
D_{k+p}	Square root of the empirical covariance matrix for predicted state vector at $k + p$
$Pr\{EOD = eod\}$	Probability of battery end-of-discharge at any future time instant eod
$i(k)$	Battery discharge current, measured in amperes at time k
$v(k)$	Battery voltage, measured in volts at time k
Δt	Sampling time, measured in seconds
$x_1(k)$	Internal impedance estimate at time k
$x_2(k)$	State of charge estimate at time k
E_{crit}	Maximum nominal energy delivered by the energy storage device
ω_1	Process noise (state transition equation)
ω_2	Process noise (state transition equation)
η	Measurement noise
Z_p	Internal battery impedance
$v_{oc}(k)$	Open circuit voltage at time k
v_o	Open circuit voltage when the battery is fully charged

I. INTRODUCTION

EVERY type of electronic device requires a power source to work properly. Common gadgets such as notebook computers, tablets, smartphones, or even more sophisticated equipment such as medical devices, robots, and satellites are also typically powered by some type of energy storage device (ESD). Nowadays, it has been proven that lithium-based ESDs offer a higher charge density by unit of mass (or volume) when compared to other combinations such as Ni-MH, Ni-Cd, or lead-acid. Also, Lithium-Ion (Li-Ion) batteries offer a longer life cycle, and a limited self-discharge rate [1], [2].

The intensive use of Li-Ion ESDs in the electric automotive industry has popularized the concept of battery management systems [3]. These systems are mainly aimed at tasks such as providing real-time information, reducing battery charging times, maximizing the amount of operating cycles, maximizing the usage time associated to the discharge cycle, maintaining the operation of all cells within their rated limits, and compensating for cell imbalance, among others. To accomplish these tasks, battery management systems must use information about the battery's State-of-Charge (SOC) [2], [3]and its remaining useful life [4]; the latter is usually expressed in terms of the State-of-Health [1], [3], [5].

SOC [2], [3], [5], [6], [8]–[13]is an indicator that represents the amount of energy that is currently available in any given ESD. The knowledge of this state variable is essential to ensure optimal path-planning in autonomous electric vehicles, as well as in any other application where it can be used as an indicator of the system's autonomy. In the particular case of Lithium-Ion batteries, SOC estimation and prognostic strategies [2], [3], [5]–[17]are fundamental for the characterization of the End-of-Discharge (EOD) time. However, as in many other state estimation problems, the SOC is not observable, and it has to be inferred from indirect but statistically related measurements [3], [9]–[13](e.g., battery voltage, discharge current, or temperature). Different structures have been proposed to characterize the battery behavior for SOC estimation purposes, including empirical models, stochastic models, and electrochemical models. The use of electrochemical models is computationally demanding in real-time applications because they require a large number of parameters [3], [6]. Open-circuit voltage (OCV) models [12]offer a simpler choice, but unfortunately their tuning requires large resting periods for the battery in the middle of its operation [3], [6], [11]–[13]. Electrochemical Impedance Spectroscopy (EIS) models [3], [8], [13]stand out as an alternative, but the equipment needed for data acquisition purposes is expensive, and sometimes very noisy [14], [18]. Current research efforts have put significant attention on the use of empirical models [2], [3], [5], [6], [10], [15], [17], [19]because of their flexibility, and the fact that they deal better with limited, noisy data. In this context, there are several approaches currently available in literature: impulse response methods [2], fuzzy logic [5], neural networks [3], [6], [10], [15], linear parameter varying system techniques [17], and support vector machines [19].

In this article, we will focus on Bayesian models. Numerous contributions have adopted stochastic filtering techniques for SOC estimation such as the Kalman filter [7], [16], the unscented Kalman filter [20], the extended Kalman filter [6], [21], and the unscented particle filter [22]. Particularly, the family of sequential Monte Carlo (SMC) methods have shown to be very effective in the process of incorporating model non-linearities, as well as complex forms of uncertainty in acquired measurements [1], [4], [11], [14], [18], [23]. One of the main advantages of SMC methods, also referred to as particle filters (PF) [24]–[26], is that they provide a clean characterization of the uncertainty in the filtering stage, which is instrumental to define risk functions associated with the SOC or EOD prognosis task. On the negative side, Bayes-based prognostic methods are very sensitive to the initial state conditions of the state-space model, and hence the performance (accuracy and precision) of the SOC estimator plays a major role in the development of long-term predictors. Although some recent developments have already used a combination of simplified electrochemical models and SMC methods to estimate the SOC of a battery [27], the problems of SOC and EOD prognosis remain interesting challenges for the prognostic and health management community.

Predicting a time threshold for safe device utilization is a challenging problem. Whether the scope is industrial, automotive, or military applications, we encounter some ubiquitous considerations that apply in real operation conditions. First, the energy left in the battery is at best poorly known. Second, the future operating profile is also uncertain. In this paper, we use a novel PF-based approach to deal with these issues, and to characterize the EOD of Li-Ion batteries. In its filtering stage, the PF algorithm handles uncertain initial conditions (which may be associated with usage, age, or battery degradation processes). This algorithm also provides for the initialization of the prognostic stage. Then, and in combination with a Markov Chain (MC) characterization of future battery operation, we obtain accurate, precise results for the EOD.

It is only natural that very different validation data sets have to be considered to test our methodology. Specifically, in this case, we extract voltage and current measurements from one Li-Ion 26650 cell and two Li-Ion 18650 cells, considering different discharge conditions. Three application scenarios are investigated. At one end of the required power spectrum, we have a four-wheel ground robot that goes though different discharge profiles due to changing terrain conditions. In this case, the discharge profile is quasi-stationary. Then, a realization of a two-state MC is tested. The states of this profile represent a constant discharge consumption of 1 ampere, and 3 amperes respectively, with transition probabilities $p_{11} = p_{21} = 0.55$, $p_{12} = p_{22} = 0.45$. The final data set considers an aggressive-power requirement, which is common for battery packs in electric vehicle applications. In this case, a Federal Urban Driving Schedule (FUDS) is used to generate the discharge current use profile.

This paper is organized as follows. Section II discusses PF algorithms for estimation and prognosis. We also define the EOD probability density function (PDF) by fusing information about long-term predictions and system hazard zones. Section III presents a novel state-space model for ESDs. Based on battery phenomenology, it requires only a minimum number of parameters, and thus is the preferred choice for online

discharge prognosis. The data sets from three different Li-Ion batteries are also presented here. Section IV deals with the problem of characterizing future discharge profiles using a two-state MC. In Section V, we present our results, which cover a wide range of power requirements from the batteries. The PF-based methodology is validated by obtaining precise EOD estimates. Section VI summarizes the conclusions.

II. Particle-Filtering-Based Prognosis Framework for Faulty Dynamic Nonlinear Systems

PF are a class of algorithms designed to obtain samples from a *target* state probability distribution $\pi_k(x_{0:k})$ sequentially. These methods are aimed at generating a set of $N \gg 1$ weighted particles $\{w_k^{(i)}, x_{0:k}^{(i)}\}_{i=1...N}, w_k^{(i)} > 0, \forall k \geq 1$, such that [24], [25]

$$\sum_{i=1}^{N} w_k^{(i)} \varphi_k \left(x_{0:k}^{(i)} \right) \underset{N \to \infty}{\longrightarrow} \int \varphi_k(x_{0:k}) \pi_k(x_{0:k}) dx_{0:k}, \quad (1)$$

in probability, and where φ_k is any π_k-integrable function. Typically, the target distribution is chosen as $\pi_k(x_{0:k}) = p(x_{0:k}|y_{1:k})$, the posterior PDF of the state vector, conditional to noisy observations $y_{1:k}$ [25].

As in any Bayesian processor, the estimation procedure involves two main stages: *prediction*, and *update*. In the prediction stage, the state vector paths $x_{0:k-1}$ are extended using an arbitrary importance distribution $q(\tilde{x}_{0:k}|x_{0:k-1})$, where $\tilde{x}_{0:k} = (x_{0:k-1}, \tilde{x}_k)$. In the update stage, the new weights $w_k^{(i)}$ are evaluated from the measurement likelihood as $w_k^{(i)} \propto w_{k-1}^{(i)} \cdot p(y_k|\tilde{x}_{0:k}) \cdot p(\tilde{x}|x_{0:k-1})/q(\tilde{x}_{0:k}|x_{0:k-1})$, where $\Sigma_{i=1}^{N} w_k^{(i)} = 1$. The most basic PF implementation, the sequential importance sampling particle filter, assumes that $p(\tilde{x}_k|x_{0:k-1}) = q(\tilde{x}_{0:k}|x_{0:k-1})$. This procedure generates an empirical representation [25] of the target distribution

$$\tilde{\pi}_k^N(x_{0:k}) = \sum_{i=1}^{N} w_{0:k}^{(i)} \delta \left(x_{0:k} - \tilde{x}_{0:k}^{(i)} \right). \quad (2)$$

The efficiency of the procedure improves as the variance of the particle weights is minimized [25].

Prognosis [28], and thus the generation of long-term prediction, is a problem that goes beyond the scope of filtering applications (because it involves the characterization of future uncertainty sources). The implementation of PF-based prognostic algorithms [29], [31] requires a procedure to propagate the uncertainty associated to the current estimate of the state PDF throughout time, assuming no new measurements are acquired. Failure prognosis algorithms always assume a nonlinear dynamic model that describes the evolution of (at least) one feature representing a measure of the severity of the fault condition (fault dimension [32]). Thus, the propagation of the uncertainty associated to the estimate of the system health condition is performed through the generation of p-step-ahead predictions. These predictions use the current particle population as the initial condition, and kernel functions to characterize the uncertainty associated to each state transition, as shown in (3).

$$\tilde{p}(x_{k+p}|\tilde{x}_{1:k+p-1}) = \sum_{i=1}^{N} w_{k+p-1}^{(i)} K\left(x_{k+p} - E\left[x_{k+p}^{(i)}|\tilde{x}_{k+p-1}^{(i)} \right] \right), \quad (3)$$

where $K(\cdot)$ is a kernel density function, which may be chosen as the process noise or a rescaled version of Epanechnikov kernels [4], [23], [29]. Furthermore, we use a regularized version of this PF-based approach that characterizes the distribution of the predicted state vector by the position of the particles instead of their weights. As a result, the predicted state PDF in the time instant $k + p$ is always represented by N particles $x_{k+p}^{(i)*} = x_{k+p}^{(i)} + h_{opt}D_{k+p}\varepsilon^{(i)}, (i = 1, \ldots, N)$, where h_{opt} is the optimal bandwidth of the kernel $K(\cdot)$, D_{k+p} is the square root of the empirical covariance of the predicted state in $k + p$, and $\varepsilon^{(i)}$ is sampled according to $\varepsilon^{(i)} \sim K$ (more details can be found in [4]). The PDF for the remaining useful life of the faulty system, or equivalently its Time-of-Failure, can then be computed by combining information from these long-term predictions and system hazard zones (areas of the state space that are associated with critical conditions for the system) [33], [34]. Focusing on the analysis of the EOD [18], the hazard zone may be characterized as a threshold for the SOC. Thus, the probability of failure at any future time instant $k = eod$ (namely the EOD probability distribution) is given by the expression [4]

$$\Pr\{EOD = eod\} = \sum_{i=1}^{N} \Pr \left(Failure|X = x_{eod}^{(i)*} \right) \cdot w_{eod}^{(i)}. \quad (4)$$

The conditional EOD probability distribution (4) assumes that a particle $x_{eod}^{(i)*}$ represents a failure condition with probability 1 when its realization for the second state (SOC value) is smaller than a given threshold.

III. State-Space Model for State-of-Charge Estimation in ESDs

Online discharge time prognosis requires an adequate characterization of the ESD model, and information on future battery operating conditions. This section focuses on the first of these tasks: the proposal of a model that characterizes the impact of different discharge currents on the battery voltage, conditional to a given SOC. We offer a prognostic-oriented solution that estimates a minimum number of parameters, thus helping to improve the accuracy and precision of the resulting EOD estimates. We did not consider models based on electrochemical characterization because they need to estimate numerous parameters (affecting the observability of the state vector), require extremely precise measurements for on-line implementation, and represent a high computational cost. Models based on EIS measurements were discarded for similar reasons.

Our solution is based on an empirical state-space model that is inspired on electric equivalent circuits for the battery cell. Previous research efforts have also used a state-space representation to describe the SOC evolution in time. In [35], the proposed state-space model uses the traditional definition for SOC (based on the battery capacity), and assumes a known look-up table to characterize the OCV curve. In contrast, an energy-based definition for the SOC is used in [36], although the parameterization that is proposed for the OCV curve is insufficient for large battery packs.

This article considers the SOC as a measure of the battery's remaining energy. More specifically, for all practical purposes,

we assume that the SOC represents a percentage of the maximum amount of energy that can be stored in the battery. This subtle change from the usual definition is motivated mainly by two facts. First, we believe that the concept of energy allows us to efficiently fuse information from battery voltage and current sensors into a single state by using the law of conservation of energy. Second, this change is necessary to adequately prognosticate the autonomy of electromechanical equipment because all algorithms should characterize future consumption in terms of the electrical power demand. Indeed, as the battery voltage drops in a nonlinear manner with respect to the SOC, the electrical power is not proportional to the battery current. Thus, a definition of SOC in terms of ampere-hours becomes insufficient in this context.

We also propose a state-space model that incorporates an improved version of the OCV curve presented in [36] as the system measurement equation. It is important to note that this new model provides an adequate representation of the dynamics associated to the measured battery discharge voltage, in contrast to the previous representation that assumed a constant value for the open-circuit voltage for a wide range of SOC values. We assume a discrete-time characterization for the battery dynamics, and the availability (real-time) of voltage and discharge current measurements (5)–(7). The structure of the proposed state-space model offers a modification to the observation equation (7) that incorporates most of the nonlinearities found in Li-Ion open-voltage discharge curves, while simultaneously enabling the implementation of reliable off-line estimation procedures for the estimation of all of its parameters.

State transition model:

$$x_1(k+1) = x_1(k) + \omega_1(k) \tag{5}$$
$$x_2(k+1) = x_2(k) - v(k) \cdot i(k) \cdot \Delta t \cdot E_{crit}^{-1} + \omega_2(k) \tag{6}$$

Measurement equation:

$$v(k) = v_L + (v_0 - v_L) \cdot e^{\gamma \cdot (x_2(k) - 1)} + \alpha \cdot v_L \cdot (x_2(k) - 1) + \cdots$$
$$\cdots (1 - \alpha) \cdot v_L \cdot \left(e^{-\beta} - e^{-\beta \sqrt{x_2(k)}} \right) - i(k) \cdot x_1(k) + \eta(k) \tag{7}$$

The discharge current $i(k)$ (measured in amperes), and the sample time Δt (measured in seconds) are input variables; and the battery voltage $v(k)$ (measured in volts) is the system output. The quantities, v_L, α, β, and γ are model parameters to be estimated off-line. The states are defined as $x_1(k)$ (unknown model parameter), and $x_2(k)$ (SOC, remnant battery energy normalized by the parameter E_{crit}). E_{crit} is the expected total energy delivered by the ESD (that could be inferred from the nominal capacity or discharge curves included in datasheets). Process (ω_1 and ω_2) and measurement (η) noises are assumed Gaussian. It is important to mention that process noise ω_2 is correlated with η, the measurement noise, because the evolution in time of state x_2 depends on voltage measurements.

The concept of *artificial evolution* [4], [26] has been applied to estimate the instantaneous absolute value of the battery internal impedance. This concept is implemented by extending the dimension of the state vector, and associating its first component (x_1) with the value of this time-varying parameter. *Artificial evolution* allows the implementation of outer feedback
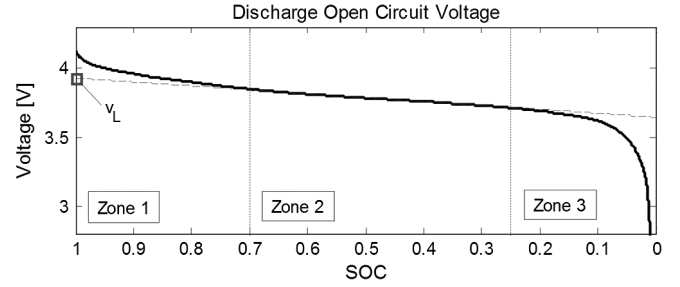

Fig. 1. Li-ion cell discharge open circuit voltage (dark black line) and linear zone projection (thin segmented line) as a function of SOC (reversed x-axis).

correction loops for parameter adaptation [29], a procedure that permits us to manipulate the variance of the process noise ω_1 to diminish the bias in Bayesian state estimates. This particular procedure has proved to be efficient because it incorporates the effect of environmental factors (e.g., temperature, or battery degradation and age). As the experimental setup did not include temperature probes, the Bayesian processor requires an adaptation strategy to infer the effect of environmental temperature changes on the internal battery impedance. The concept of *artificial evolution* plays an important role in that process.

Other available models (see Section I) incorporate a large number of parameters, increasing the complexity of the online estimation and prognosis stages. In contrast, (7) has only a few parameters, and closely represents the typical behavior that can be found in OCV vs. SOC curves of Li-Ion batteries (see Fig. 1). Furthermore, our methodology allows obtaining the parameters associated with the measurement equation (7) solely using information from a single, prior discharge test. This test (training data) is mainly used for offline estimation of parameters, v_0, v_L, α, β, and γ in (7), as well as the characterization of the *prior* distribution for $x_1(0)$.

Equation (7) considers that the OCV curve has three different zones that require proper characterization, as shown in Fig. 1. In the first zone, the OCV curve shows an exponential decay as the SOC diminishes from a fully-charged condition to approximately 70%. In the second zone, the OCV basically presents an affine relationship with respect to the SOC (SOC between 70% and 25%). The third zone is characterized by an abrupt voltage drop with respect to small decrements in the SOC value. As the OCV curve is basically approximated as the sum of the voltage measured at battery terminals and a voltage drop caused by the battery internal impedance, the state-space model would become unobservable if all discharge tests were to consider constant currents. For this reason, we characterize the OCV curve using data from tests where at least two pulses are added to the battery discharge current. These pulses can be implemented at arbitrary time instants, as long as they take place inside Zone 2 (where the OCV-SOC relationship is linear; see Fig. 2(a)). This experimental procedure can be easily implemented by approximating the *Ecrit* parameter as the nominal battery energy. The purpose of these pulses is to estimate the absolute value of the internal impedance from the expression $|Z_p| = |\Delta V / \Delta I|$, assuming $v_{oc}(k) = v(k) + i(k) \cdot |Z_p|$, where $v(k)$ is the voltage
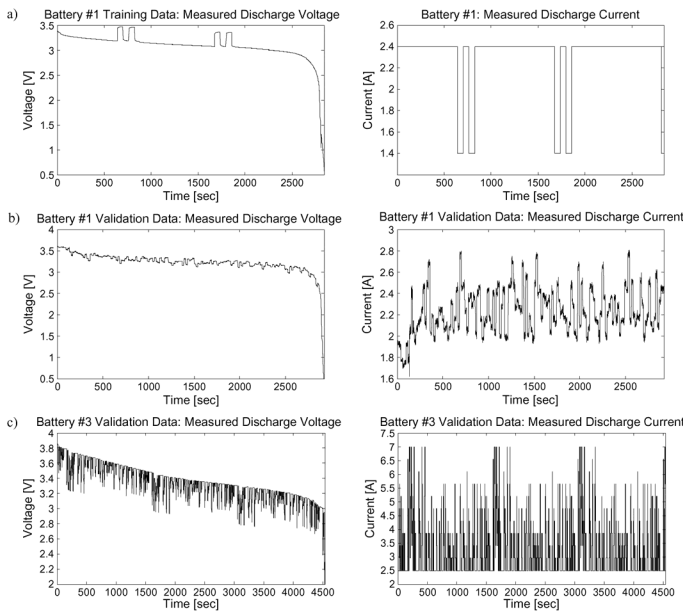
Fig. 2. Measured voltage and current discharge data for Li-Ion cells: (a) model identification test for Battery #1, (b) validation data set for Battery #1, and (c) validation data set for Battery #3.

measured at the terminals of the battery at time k, Z_p is the internal battery impedance, and $v_{oc}(k)$ is the open-circuit voltage at time k.

Once $v_{oc}(k)$ and the internal impedance approximation for $|Z_p|$ are obtained using the aforementioned procedure, it is possible to estimate (off-line) the parameters that define the structure of (7). To do this estimate, the voltage discharge curve in Zone 2 is first modeled as $v_L + \alpha \cdot v_L$ (SOC—1), where $\alpha \cdot (v_L$ is the curve slope, and v_L is the y-intercept of the curve when considering a reverse SOC axis (SOC $= 1$, fully charged battery); see Fig. 1. Although this affine representation is sufficient to characterize Zone 2, a complete representation of the OCV discharge curve for the whole SOC range requires us to incorporate additional terms to characterize Zones 1 and 3. Thus, for SOC values close to 1, the OCV curve includes the term $(v_0 - v_L)^{e^{\gamma \cdot (SOC-1)}}$, where v_0 is the OCV when the battery is fully charged (a value that can be easily measured before performing the test), and the parameter γ may be obtained by minimizing the mean squared error with respect to the measured OCV curve in Zone 2. Finally, to represent the abrupt voltage drop that occurs at low SOC values, it is necessary to add the term, where β minimizes the mean squared error in Zone 3 with respect to the voltage measured in the battery terminals during discharge.

Three different Li-Ion batteries were used to validate the efficacy of the proposed off-line parameter estimation methodology, as well as the capability of the model structure to characterize the battery discharge voltage curve. Training data were collected by implementing the discharge profile at a nominal constant current that is illustrated in Fig. 2(a)). Cells used on these experiments were discharged until the voltage dropped to 0.5 volts, although the manufacturer recommends to operate them with a safety lower voltage of 2.8 volts. In real applications, either for safety reasons or constant-power load require-

TABLE I
MODEL PARAMETERS FOR BATTERIES #1 AND #2

Battery	α	β	γ	v_0	v_L	E_{crit}	Z_p
1	0.08	16	19.65	4.12	3.987	20127	0.30
2	0.15	12	6.61	4.00	3.813	19865	0.20
3	0.15	17	10.50	4.14	3.997	46858	0.12

ments, the high voltage drop that occurs at low SOC values may not be reached. However, for identical reasons, model errors for that specific operating zone may not be relevant.

Validation data set #1 (see Fig. 2(b)) is obtained from a Li-Ion 18650 cell (3.7 volts, 2.4 ampere-hours) that is discharged with a profile that emulates the operation of a four-wheel ground robot [37], where the maximum, and minimum current values were defined as 2.809 amperes, and 1.619 amperes, respectively. Validation data set #2 corresponds to a discharge test for a Li-Ion 18650 cell (3.7 volts, 3 ampere-hours), where the battery current discharge profile is computed as a realization of a two-state Markov chain with transition probabilities $p_{11} = p_{21} = 0.55$, $p_{12} = p_{22} = 0.45$, and where the states are defined in terms of the discharge current value (state #1, 1 ampere; state #2, 3 amperes). Validation data set #3 (See Fig. 2(c)) is obtained from a LiNiCoMn 26650 cell (3.7 volts, 4 ampere-hours) that is discharged with a profile that corresponds to an adaptation of the FUDS test [38]. This test adaptation assumes that the lowest discharge current is 2.5 amperes, and that the maximum discharge current is 7 amperes (the latter representing 100% discharge power). For every discharge power datum P_{FUDS} (measured as a percentage of the maximum discharge power), the test computes the corresponding discharge current value I_{FUDS} as $I_{FUDS} = 0.045 \cdot P_{FUDS} + 2.5$. As can be seen in Fig. 2(c), the proposed discharge profile covers a wide range of current values. Table I shows the parameters obtained for each battery using the proposed methodology.

IV. STATISTICAL CHARACTERIZATION OF USE PROFILES IN ESDs, AND IMPLEMENTATION ISSUES RELATED TO PF-BASED PROGNOSTIC ALGORITHMS

This section provides an analysis of the aspects that should be considered in a statistical characterization of future discharge profiles. Also, some important considerations to be followed in the implementation of PF-based frameworks for SOC prognosis are studied, including the accuracy of EOD expectation, and the Just-In-Time Point (JITP) [28].

A. Statistical Characterization of Future Battery Discharge Current Profiles

The large uncertainty associated with the problem of EOD prognosis has at least two main sources. On the one hand, the uncertainty of the current state estimate has to be propagated in time according to the state transition model (5), (6). As a result, even if the future battery use profile is known, the EOD must be defined as a random variable. On the other hand, the future discharge profile is unknown in practical applications. Fortunately, the implementation of particle-filtering-based prognostic methods [4], [18], [23], [29]–[32] allows us to define the *prior*

distribution of system input variables in terms of empirical distributions, which can afterwards be fused with information of state PDF estimates to generate long-term predictions. However, we propose a slightly different approach, where the discharge profile that was applied to the battery in the recent past is considered as a realization of a two-state Markov chain. In this statistical characterization, one of the states of the Markov chain represents a high-energy consumption profile, while the second state is related to low-energy consumption profiles. Once the Markov chain is properly defined, which is equivalent to estimating the most appropriate values for maximum and minimum discharge currents and all transition probabilities, it can be used to generate several (equally probable) realizations of future discharge profiles. Each of these profiles can be then used as future system inputs within the particle-filtering-based prognostic framework to generate a PDF estimate for the EOD. As a result, and using the law of total probability, it is possible to fuse information from both the system state estimate and the most probable utilization profiles to prognosticate the EOD.

The implementation of this prognostic method requires the estimation of transition probabilities, and the definition of maximum and minimum discharge currents. For example, if it is assumed that the battery is energizing electro-mechanical systems and providing relatively constant power, the average value of the current will tend to increase as the SOC decreases (because the battery voltage also decreases). This tendency makes it essential to include adaptation schemes that could learn (from acquired data) the most representative values for high and low energy consumption states.

The statistical characterization of battery discharge data considers a segmentation of all acquired current measurements in regular time intervals. Each interval contains a fixed number of samples N_w, as shown in Fig. 3. This segmentation generates m time intervals such that $m\lfloor L/N_w \rfloor$, where L is the number of measurements available at the moment. For simplicity, if the ratio between the number of measurements and N_w is not an integer, then the first window can include more data samples. A low-pass filter is applied to the discharge current data to discard outliers and anomalous peaks, obtaining a filtered signal $i'(k)$ as a result. Then, for each jth interval $(j = 1 \ldots m)$, we compute the minimum and maximum discharge current values, $i_{low}^{(j)} = \min\{i'(k)\}$, and $i_{high}^{(j)} = \max\{i'(k)\}$, where $k = 1 \ldots N_w$ is a time index valid within the jth window. Next, on each interval, current measurements are quantized into two possible values defined by $i_{low}^{(j)}$, and $i_{high}^{(j)}$. These values define the low-energy, and high-energy consumption states of the Markov Chain that characterizes the jth interval. Discharge current data satisfying $i' > (i_{high}^{(j)} + i_{low}^{(j)})/2$ are quantized as $i_{high}^{(j)}$; otherwise, they are quantized as $i_{low}^{(j)}$. For each interval, it is possible to compute transition probabilities p_{ij} between low-energy and high-energy consumption states. These transition probabilities are estimated through maximum likelihood [39], [40], obtaining the estimator $\hat{p}_{ab}^{(j)} = n_{ab}^{(j)}/\Sigma_k n_{ak}^{(j)}$ (where n_{ab} corresponds to the number of transitions from state a to state b in the jth interval). The minimum number of samples N_w to be included in any interval should allow us to attain a maximum likelihood estimator for the transition probabilities.
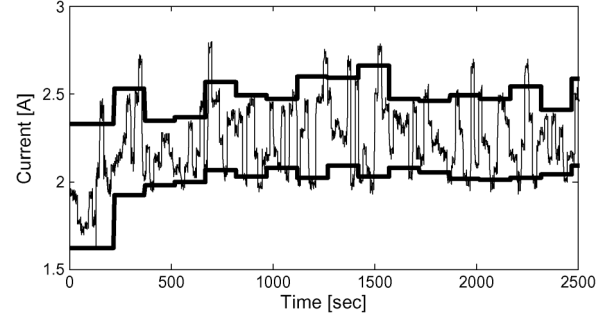

Fig. 3. Example of characterization of maximum and minimum discharge current levels for future operation of the ESD based on exponentially weighted moving average algorithms.

To incorporate information about how the battery was used before the mth time interval, an adaptation scheme is implemented by using an exponentially weighted moving average (EWMA) [41] to compute the two values, $\tilde{i}_{low}^{(j)}$ and $\tilde{i}_{high}^{(j)}$, that define the states of the Markov chain that will be used to characterize the discharge profile during the prediction stage:

$$\tilde{i}_{low}^{(j)} = (1 - \lambda)i_{low}^{(j)} + \lambda\tilde{i}_{low}^{(j-1)} \quad (j = 2 \ldots m), \quad (8)$$

$$\tilde{i}_{high}^{(j)} = (1 - \lambda)i_{high}^{(j)} + \lambda\tilde{i}_{high}^{(j-1)} \quad (j = 2 \ldots m). \quad (9)$$

The parameter $\lambda = 0.65$ corresponds to the forgetting factor of the EWMA algorithm. The EWMA is also applied to the transition probabilities. As a result of the adaptation scheme, the prognostic module solely considers the low and high current values, and the transitions probabilities of the last time interval m. This method may be extended to a multiple-state Markov Chain.

B. Implementation Issues: PF-Based Discharge Time Prognosis Framework

The formulation of PF-based prognostic approaches has been widely covered in literature [1], [4], [14], [23], [29], [31]. However, there are specific issues associated to the implementation of these schemes that depend, in a strong manner, on the number of states of the dynamic system, and the type of nonlinearities exhibited by them. For this reason, it is important to determine the best algorithm parameters that should be used in prognostic applications oriented at SOC monitoring in ESD, and predictions about the EOD time. More specifically, it is important to focus on the number of particles that needs to be considered to represent the state PDF on each realization of the stochastic predictive model, as well as the number of realizations of the filtering algorithm that are required to ensure standards in terms of accuracy of the predicted EOD PDF. Similarly, it is important to analyze the number of realizations of the MC that are required for an adequate characterization of different future ESD discharge profiles, always considering that each realization of the MC corresponds to a possible future usage of the ESD through a sequence of the current states.

The analytical solution of the SOC monitoring problem during a discharge in ESD may prove to be complex to obtain, due to the fact that the process is non-linear and non-Gaussian. In this regard, the utilization of a simplified scenario, where the

TABLE II
EFFECT OF NUMBER OF PF REALIZATIONS ON $JITP_{\gamma\%}$ VALUE (MEASURED IN SECONDS), USING 40 PARTICLES IN THE BAYESIAN FILTER DESIGN

	Simplified Analytic Solution	PF-based SOC Prognosis (25 realizations of the filter)	PF-based SOC Prognosis (100 realizations of the filter)
$JITP_{5\%}$	2894	3240.6	3241
$JITP_{10\%}$	2957	3248.2	3248.6
$JITP_{50\%}$	3276	3276	3276.4

TABLE III
EFFECT OF NUMBER OF MARKOV CHAIN REALIZATIONS ON $JITP_{\gamma\%}$ VALUE (MEASURED IN SECONDS)

	Analytic Solution	PF-based SOC Prognosis 25 realizations	PF-based SOC Prognosis 50 realizations
$JITP_{5\%}$	2897	2891.7	2900.3
$JITP_{10\%}$	2960	2952.6	2963.2
$JITP_{50\%}$	3282	3257.5	3282.6

discharge is described by a linear Gaussian dynamic system, offers the opportunity to compare the performance of suboptimal PF-based SOC prognosis for ESD using the *a priori* prediction equation of the Kalman filter. For this reason, a similar procedure to the one applied in [42]is used on a battery discharge simplified model to characterize the PDF of the EOD. This comparative analysis provides information about the most appropriate values for the parameters that define the filter implementation.

Performance indicators for prognostics algorithms used in this analysis incorporate information from EOD expectations, which correspond to the instant k when the expectation of the battery SOC reaches a null condition, as well as the Just-In-Time Point value. The latter measure incorporates the concept of risk, specifying the cycle of operation where the probability of failure reaches a specified threshold γ $(JITP_{\gamma\%})$.

$$\widehat{EOD} \triangleq E\{k|E\{x_2(k)\} = 0\} \tag{10}$$

$$JITP_{\gamma\%} = \arg\min_{eod}(\Pr\{EOD \leq eod\} \geq \gamma\%) \tag{11}$$

Several experiments were conducted to test PF-based discharge time prognostic algorithms. These experiments utilized a simplified discharge model, and varied either the number of particles of the PF implementation or the number of MC realizations that are needed to characterize the uncertainty of the future discharge profile. Results were compared with the analytic solution of the simplified model in terms of the $JITP_{\gamma\%}$ value and the EOD expectation (equivalent to $JITP_{50\%}$ in symmetrical distributions) [43]. The $JITP_{\gamma\%}$ value is critical to define the number of particles that are needed to represent the uncertainty of the system because it provides information about the tails of the distribution. Also, and as explained in [42], the accuracy on the EOD expectation greatly depends on both the number of realizations for the stochastic process that defines the innovations of the PF implementation and the number of realizations of the Markov chain. This analysis helped to determine that 40 particles are appropriate for algorithm implementation purposes, if the computational cost associated to the implementation of PF estimators is also considered. In addition, as shown in Table II, 25 realizations of the PF algorithm are sufficient to provide reasonable estimates for the $JITP_{5\%}$, $JITP_{10\%}$, and $JITP_{50\%}$, conditional to the fact that 40 particles are to be used, because changes on the estimates were negligible even when using 100 realizations.

Furthermore, and following the guidelines proposed in [42], an exhaustive analysis was conducted to determine the number of MC realizations that are required to generate reliable EOD estimates, assuming the utilization of 40 particles in the PF implementation. Table III summarizes the results obtained in terms of the $JITP_{\gamma\%}$ ($\gamma = \{5, 10, 50\}$).

Note that, for more than 25 realizations of the MC that characterizes the battery future operating profile, improvements are negligible. This fact determines that 25 realizations of the implemented MC are adequate, conditional to the fact that the implementation of the PF-based prognostic algorithm uses 40 particles and 25 realizations of the Bayesian filter to characterize the uncertainty associated to the state.

V. PARTICLE-FILTERING-BASED DISCHARGE TIME PROGNOSIS FOR LITHIUM-ION ESDs

The problem of battery EOD time has been discussed by several authors in recent years. Most of them learn the trend of the discharge curve assuming that the only sources of uncertainty are associated to unknown model parameters or the estimates of the state vector, while the future operating profile is assumed to be a deterministic function of time (constant battery current, most of the times). This assumption is equivalent to assuming that the *a priori* probability distribution of the battery discharge profile distribution is a Dirac's delta function. Although this assumption speeds up the prognostic procedure (a desirable condition for real-time prognostic algorithms), it does not characterize changes in future operating conditions that could affect the system's autonomy. By combining a classic implementation of a particle-filtering-based prognostic framework [4], [15]with a statistical characterization of the battery use profile (Section IV), we characterize the uncertainty of future discharge profiles, and improve the accuracy of the prognostic results.

Our PF-based approach considers two stages for the generation of the EOD PDF: filtering, and prognosis. In the beginning of the filtering stage, most of the time there is no certain knowledge about the amount of energy stored in the battery. This condition implies that there is no information about the SOC and the initial condition of its associated state. To ensure its convergence to the actual SOC value during this stage, it is important to correct for errors that could be associated to inadequate initial conditions. This fact is a critical issue to guarantee an adequate initialization of the prognosis stage, which is based on the results of the filtering stage. This approach considers an adaptive learning strategy [29]that increases the uncertainty associated with the state x_2 in (6) (through the manipulation of the variance of the process noise ω_2), based on the fact that changes on the internal battery impedance (and thus the value associated to the state x_1) are negligible during a given discharge cycle [44]. Although this procedure helps to adjust the prior knowledge on the initial condition of the state vector,

TABLE IV
RESULTS FOR DIFFERENT REALIZATIONS OF THE PROPOSED PF-BASED SOC
PROGNOSIS MODULE (BATTERY #1). GROUND TRUTH EOD AT 2738 SECONDS

No.	$E\{E\hat{O}D\}$ (seconds)	95% Confidence Interval (seconds)	$JIT_{5\%}$ (seconds)	$JIT_{15\%}$ (seconds)
1	2643	[2552 ; 2741]	2572	2594
2	2751	[2612 ; 2892]	2632	2669
3	2634	[2600 ; 2669]	2600	2612
4	2670	[2533 ; 2820]	2554	2596
5	2761	[2653 ; 2876]	2675	2700

TABLE V
RESULTS FOR DIFFERENT REALIZATIONS OF THE PROPOSED PF-BASED SOC
PROGNOSIS MODULE (BATTERY #2). GROUND TRUTH EOD AT 3381 SECONDS

No.	$E\{E\hat{O}D\}$ (seconds)	95% Confidence Interval (seconds)	$JIT_{5\%}$ (seconds)	$JIT_{15\%}$ (seconds)
1	3317	[3244 ; 3390]	3237	3266
2	3324	[3249 ; 3398]	3240	3272
3	3265	[3215 ; 3314]	3174	3226
4	3287	[3215 ; 3359]	3203	3237
5	3303	[3255 ; 3350]	3246	3267

TABLE VI
RESULTS FOR DIFFERENT REALIZATIONS OF THE PROPOSED PF-BASED SOC
PROGNOSIS MODULE (BATTERY #3). GROUND TRUTH EOD AT 4283 SECONDS

No.	$E\{E\hat{O}D\}$ (seconds)	95% Confidence Interval (seconds)	$JIT_{5\%}$ (seconds)	$JIT_{15\%}$ (seconds)
1	4118	[4050 ; 4187]	4025	4059
2	4115	[4044 ; 4186]	3997	4034
3	4073	[4010 ; 4136]	3974	4005
4	4061	[4013 ; 4109]	3981	4003
5	4101	[4023 ; 4180]	4002	4038

Fig. 4. SOC prognosis for Battery #1 using the proposed PF-based framework. (a) Estimated SOC (dark black line), predicted SOC (dark black dashed line), and 95% confidence interval for SOC prediction (thin segmented line), with EOD threshold defined as 5% SOC. (b) Evolution of the state x_1, as a function of SOC, during the estimation (solid line) and prediction (dashed line) stages. (c) Measured voltage (thin black line), estimated voltage (dark black line), and predicted voltage drop (dashed dark black line), as a function of SOC.

it may incorporate artificial sources of uncertainty within the Bayesian processor if kept invariant [29]. For this reason, and after a few battery voltage and current measurements are acquired, the variance is exponentially reduced, converging to a pre-defined lower bound (which is part of the PF implementation design parameters). This procedure, which can be considered as an outer feedback correction loop [29] in a failure prognostic routine, is critical to ensure a reasonable initial condition for the state vector. Once the uncertainty associated to the state estimate has been quantified and bounded, it is possible to implement regularization [4] and kernel-based techniques within the particle-filtering-based prognostic framework to study the manner in which the state probability distribution will evolve in time (3).

Validation of the proposed approach has been performed using the data from three different Lithium-Ion cells (as described in Section III), and using performance measures (10) and (11). Validation data set #1 emulated the operation of a four-wheel ground robot. Validation data set #2 corresponds to a discharge profile computed as a realization of a two-state Markov chain. Validation data set #3 emulates and adapts the FUDS test. The ground truth EOD for the first data set, obtained from Battery #1, occurred at 2738 seconds of operation. In the case of Battery #2, the ground truth EOD is 3381 seconds. For Battery #3, the value of the ground truth EOD is 4283 seconds. The initial condition for state x_2 is arbitrarily generated as a uniform random variable [0.80, 0.90], even when it was known that in all experiments the batteries were always fully charged. The latter intended to demonstrate how well the estimation algorithm responds to erroneous initial conditions. Provided that PF-based EOD estimates are random variables, the validation analysis included several realizations of the filter for each data set. Figures will only illustrate results for one particular realization, whereas Tables IV, V, and VI aggregate information from all computed realizations.

Fig. 4 and Fig. 5 show the results of the prognostic algorithm using a (random) single realization of the PF-estimation algorithm, and one of the 25 realizations of the Markov chain that characterizes the future battery use profile according to the procedure described in Section IV-A. EOD prognosis is computed at the 1800th second of operation for Battery #1 and #2, and at the 2947th second for Battery #3. In these three cases, the proposed method and model structure allow us to quickly overcome the problem of erroneous initial conditions for state x_2, obtaining reliable estimates of the SOC in terms of the conditional expectation of the PF-based PDF estimate. Furthermore,
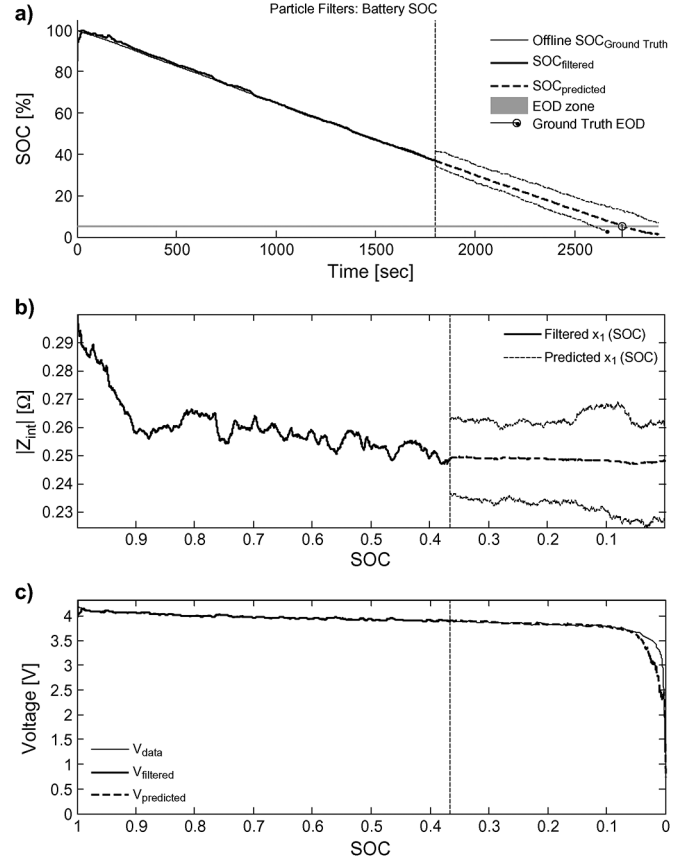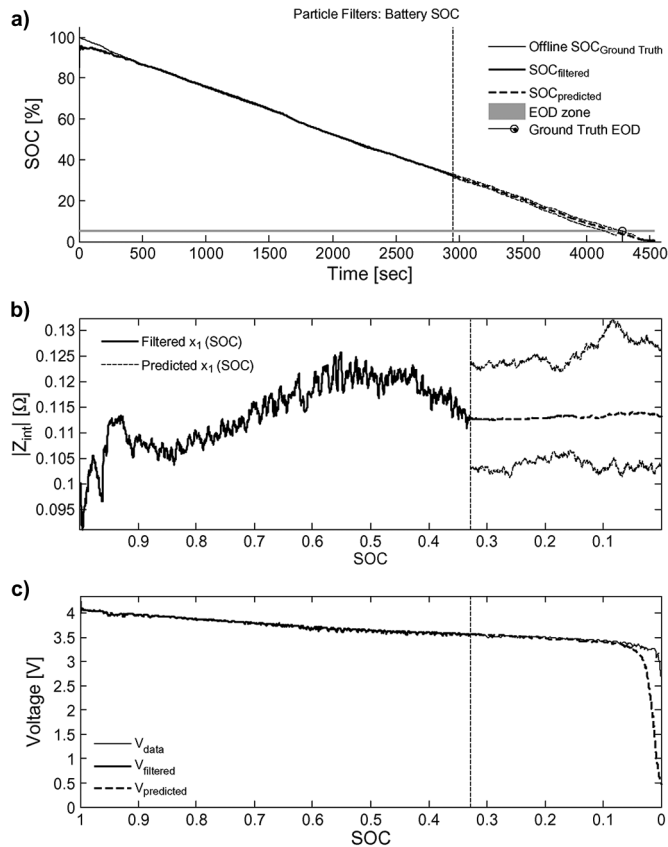
Fig. 5. SOC prognosis for Battery #3 using the proposed PF-based framework. (a) Estimated SOC (dark black line), predicted SOC (dark black dashed line), and 95% confidence interval for SOC prediction (thin segmented line), where EOD threshold is defined as 5% SOC. (b) Evolution of the state x_1, as a function of SOC, during the estimation (solid line), and prediction (dashed line) stages. (c) Measured voltage (thin black line), estimated voltage (dark black line), and predicted voltage drop (dashed dark black line), as a function of SOC.
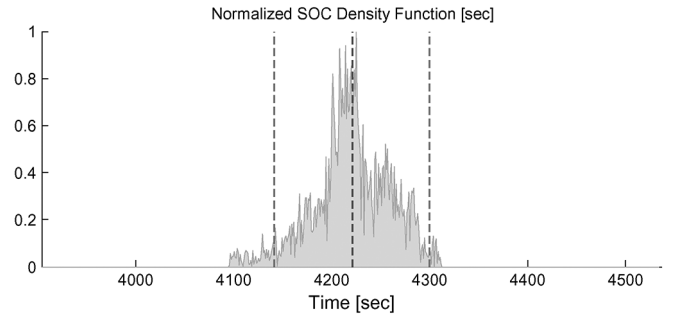

Fig. 6. EOD PDF estimate (normalized) for Battery #3. Vertical dashed lines show the PDF expectation and the limits of the 95% confidence interval. Ground truth EOD is 4283 seconds.

the predicted output voltage for Battery #1 (see Fig. 4(c)) correctly includes a characterization of the voltage drop that occurs when the SOC reaches less than 10% (even considering that this event occurs at late stages within the prediction routine). However, Fig. 5(c) shows an early voltage drop for the output voltage of Battery #3 at a SOC of 6%, due to a higher uncertainty associated to the usage profile (with respect to Batteries #1 and #2). The resulting EOD PDF estimate allows the building of 95% confidence intervals for the discharge event, assuming that the statistical characterization of the system input (discharge profile) is invariant. Although this graphical information is useful to illustrate the system autonomy, it is incomplete because it is first necessary to evaluate the response of the filter to various realizations of the innovation process. Tables IV, V, and VI present the results obtained when running at least 5 different instances of the proposed approach, considering that each instance implies a single realization of the PF algorithm to estimate the state PDF at the 1800th second of operation in the case of Battery #1 and #2, or the 2947th second of operation in the case of Battery #3, and 25 realizations of the Markov chain that characterizes the future battery use profile. These results show that the proposed method can be used to statistically quantify the effect that random changes in the battery discharge current have on the ESD SOC.

EOD estimates presented in Table IV show that the EOD expectation is, indeed, a random variable. Furthermore, it may happen that some realizations of this random variable underestimate (or overestimate) the ground truth EOD. Nevertheless, the obtained estimates (for both batteries) are sufficiently accurate. More importantly, they tend to underestimate the EOD, thus minimizing the probability of unexpected failure (conservative approach). In fact, the values obtained for the $JITP_{\gamma\%}$ in Table IV are always smaller than the ground truth EOD, thus ensuring a safety utilization of the ESD. The maximum overestimation error in the conditional expectation is only 23 seconds, over a 938 seconds prediction window. The EOD conditional expectation estimates for Battery #2, and Battery #3 are presented in Table V, and VI respectively, following a similar procedure as in the case of Battery #1. In those cases, all prognosis results provide EOD conditional expectations that underestimate the EOD ground truth. The proposed method obtained a maximum error of 116 seconds, and 222 seconds for Battery #2, and Battery #3, while the prediction horizon was 1581 seconds, and 1336 seconds, respectively. As the characterization of the future usage profile for Battery #2 is made with realizations of a two state Markov chain, the prognosis stage leads to better results compared with Battery #3. This difference produces a higher underestimation of the EOD expectation for Battery #3. Underestimation of the EOD is not critical when compared to its overestimation because the latter would lead one to make wrong decisions in terms of systems autonomy. Fig. 6 shows an illustration of the EOD PDF estimate, including the expectation and 95% confidence interval limits (ground truth EOD at 4283 seconds).

Considering the length of the long-term prediction windows, the maximum error between the ground truth and the expected EOD correspond to only 2.45%, 7.3%, and 16.6% for Battery #1, Battery #2, and Battery #3, respectively. Also, the corresponding maximum lengths for the obtained confidence intervals are 30.6%, 9.4%, and 11.8% of the prediction window. These results show that the proposed prognosis SOC framework presents a trade-off between the accuracy and precision of EOD estimates. In terms of Just-In-Time Point estimates, the maximum difference between the ground truth EOD and the $JITP_{5\%}$, and $JITP_{15\%}$ values are 184 seconds, and 142 seconds, respectively (19.6%, and 15.1% of the prediction window) for Battery #1. In the case of Battery #2, that difference is 195

seconds, and 160 seconds, respectively (12.3%, and 10.1% of the prediction window). For Battery #3, the difference is 309 seconds, and 280 seconds, respectively (23.1%, and 20.9% of the prediction window). All these results provide reliable information for decision making processes associated to the ESD autonomy.

VI. CONCLUSIONS

A particle-filtering-based SOC and EOD prognostic approach has been proposed, tested, and validated. This approach uses a statistical characterization of battery use profiles to estimate the SOC, and predict the discharge time of Li-Ion batteries. Three different lithium-ion battery cells have been used to generate experimental data, under dissimilar operating conditions, for both training and validation purposes. The first of these discharge profiles emulated the operation of a four-wheel ground robot. The second data set corresponded to a discharge profile computed as a realization of a two-state Markov chain. Finally, the third discharge profile emulated the FUDS test.

An empirical state-space model, inspired by the battery phenomenology, was also hereby introduced and validated. The model allows the implementation of Bayesian filtering methods that efficiently (and effectively) estimated SOC in real-time. Furthermore, the implementation of an outer correction loop during the filtering stage (to modify the variance of the process noise ω_2) provided quick adaptation for erroneous initial conditions. This reduced dramatically the associated impact on the EOD estimate bias.

SOC and EOD prognosis is implemented using a PF-based method that considers a statistical characterization of future discharge profiles based on maximum likelihood estimates of transition probabilities for a two-state Markov chain. Experimental results prove that the proposed framework allows us to successfully prognosticate the discharge time in terms of conditional expectations, 95% confidence intervals, and $JITP_{\gamma\%}$ points. This ability offers conservative (but accurate) EOD estimates that help to minimize the probability of unexpected failure, and ensure a safe utilization of the ESD.

REFERENCES

[1] B. Saha and K. Goebel, "Modeling li-ion battery capacity depletion in a particle filtering framework," in *Proc. Annu. Conf. Prognostics and Health Management Society*, San Diego, CA, USA, 2009.

[2] A. Ranjbar, A. Banaei, A. Khoobroo, and B. Fahimi, "Online estimation of state of charge in li-ion batteries using impulse response concept," *IEEE Trans. Smart Grid*, vol. 3, no. 1, pp. 360–367, Mar. 2012.

[3] B. Pattipati, C. Sankavaram, and K. Pattipati, "System identification and estimation framework for pivotal automotive battery management system characteristics," *Trans. Syst., Man, Cybern. C: Applicat. Rev.*, vol. 41, pp. 869–884, 2011.

[4] M. Orchard and G. Vachtsevanos, "A particle-filtering approach for on-line fault diagnosis and failure prognosis," *Trans. Inst. Meas. Control 2009*, vol. 31, pp. 221–246, 2009.

[5] A. J. Salkind, C. Fennie, P. Singh, T. Atwater, and D. Reisner, "Determination of state-of-charge and state-of-health of batteries by fuzzy logic methodology," *J. Power Sources*, vol. 80, pp. 293–300, 1999.

[6] M. Charkhgard and M. Farrokhi, "State-of-charge estimation for lithium-ion batteries using neural networks and EKF," *IEEE Trans. Ind. Electron.*, vol. 57, no. 12, pp. 4178–4187, Dec. 2010.

[7] D. Vinh Do, C. Forgez, K. El Kadri Benkara, and G. Friedrich, "Impedance observer for a li-ion battery using Kalman filter," *IEEE Trans. Veh. Technol.*, vol. 58, no. 8, pp. 3930–3937, Oct. 2009.

[8] L. Ran, W. Junfeng, W. Haiying, and L. Gechen, "Prediction of state of charge of Lithium-ion rechargeable battery with electrochemical impedance spectroscopy theory," in *Proc. 2010 5th IEEE Conf. Industrial Electronics and Applications (ICIEA)*, Jun. 2010, pp. 684–688.

[9] D. Cadar, D. Petreus, and C. Orian, "A method of determining a lithium-ion battery's state of charge," in *Proc. 15th Int. Symp. Design and Technology of Electronics Packages (SIITME) 2009*, Sep. 2009, pp. 257–260.

[10] S. Qingsheng, Z. Chenghui, C. Naxin, and Z. Xiaoping, "Battery state-of-charge estimation in electric vehicle using Elman neural network method," in *Proc. 29th Chinese Control Conf. (CCC) 2010*, Jul. 2010, pp. 5999–6003.

[11] Z. Di, M. Yan, and B. Qing-Wen, "Estimation of Lithium-ion battery state of charge," in *Proc. 30th Chinese Control Conf.*, Jul. 2011.

[12] X. Tang, X. Mao, J. Lin, and B. Koch, "Li-ion battery parameter estimation for state of charge," in *Proc. Amer. Control Conf. (ACC) 2011*, Jun.–Jul. 2011, pp. 941–946.

[13] J. Xu, C. Mi, B. Cao, and J. Cao, "A new method to estimate the state of charge of lithium-ion batteries based on the battery impedance model," *J. Power Sources*, vol. 233, pp. 277–284, Jul. 2013.

[14] M. Dalal, J. Ma, and D. He, "Lithium-ion battery life prognostic health management system using particle filtering framework," *Proc. Inst. Mech. Eng. Part O: J. Risk Rel.*, vol. 225, pp. 81–90, 2011.

[15] N. Watrin, B. Blunier, and A. Miraoui, "Review of adaptive systems for lithium batteries state-of-charge and state-of-health estimation," in *Proc. 2012 IEEE Transportation Electrification Conf. Expo (ITEC)*, 2012.

[16] H. Dai, X. Wei, Z. Sun, J. Wang, and W. Gu, "Online cell SOC estimation of Li-ion battery packs using a dual time-scale Kalman filtering for EV applications," *Appl. Energy*, vol. 95, pp. 227–237, 2012.

[17] Y. Hu and S. Yurkovich, "Battery cell state-of-charge estimation using linear parameter varying system techniques," *J. Power Sources*, vol. 198, pp. 338–350, 2012.

[18] B. Saha, K. Goebel, S. Poll, and J. Christophersen, "Prognostics methods for battery health monitoring using a Bayesian framework," *IEEE Trans. Instrum. Meas.*, vol. 58, no. 2, pp. 291–296, 2009.

[19] J. Alvarez Anton, P. Garcia Nieto, C. Blanco Viejo, and J. Vilan Vilan, "Support vector machines used to estimate the battery state of charge," *IEEE Trans. Power Electron.*, vol. 28, no. 12, pp. 5919–5926, Dec. 2013.

[20] S. Santhanagopalan and R. White, "State of charge estimation using an unscented filter for high power lithium ion cells," *Int. J. Energy Res.*, vol. 34, no. 2, pp. 152–163, 2010.

[21] C. Hu, B. Youn, and J. Chung, "A multiscale framework with extended Kalman filter for lithium-ion battery SOC and capacity estimation," *Appl. Energy*, vol. 92, pp. 694–704, 2012.

[22] Y. He, X. Liu, C. Zhang, and Z. Chen, "A new model for state-of-charge (SOC) estimation for high-power Li-ion batteries," *Appl. Energy*, vol. 101, pp. 808–814, 2013.

[23] M. Orchard, L. Tang, B. Saha, K. Goebel, and G. Vachtsevanos, "Risk-sensitive particle-filtering-based prognosis framework for estimation of remaining useful life in energy storage devices," *Stud. Informat. Control*, vol. 19, pp. 209–218, 2010.

[24] M. Arulampalam, S. Maskell, N. Gordon, and T. Clapp, "A tutorial on particle filters for online nonlinear/non-Gaussian Bayesian tracking," *IEEE Trans. Signal Process.*, vol. 50, no. 2, pp. 174–188, Feb. 2002.

[25] C. Andrieu, A. Doucet, and E. Punskaya, *Sequential Monte Carlo Methods for Optimal Filtering*, A. Doucet, N. de Freitas, and N. Gordon, Eds. New York, NY, USA: Springer-Verlag, 2001, Sequential Monte Carlo Methods in Practice.

[26] J. Liu and M. West, "Combined parameter and state estimation in simulation-based filtering," in *Sequential Monte Carlo Methods in Practice*, A. Doucet, N. de Freitas, and N. Gordon, Eds. New York, NY, USA: Springer-Verlag, 2001.

[27] M. Samadi, S. Alavi, and M. Saif, "An electrochemical model-based particle filter approach for Lithium-ion battery estimation," in *Proc. 51st IEEE Conf. Decision and Control*, Dec. 2012.

[28] S. Engel, B. Gilmartin, K. Bongort, and A. Hess, "Prognostics, the real issues involved with predicting life remaining," in *Proc. 2000 IEEE Aerospace Conf.*, 2000, vol. 6, pp. 457–469.

[29] M. Orchard, F. Tobar, and G. Vachtsevanos, "Outer feedback correction loops in particle filtering-based prognostic algorithms: Statistical performance comparison," *Stud. Informat. Control*, vol. 18, pp. 295–304, Dec. 2009.

[30] D. Edwards, M. Orchard, L. Tang, K. Goebel, and G. Vachtsevanos, "Impact of input uncertainty on failure prognostic algorithms: Extending the remaining useful life of nonlinear systems," in *Proc. Annu. Conf. Prognostics and Health Management Society 2010*, Oct. 2010.

[31] C. Chen, G. Vachtsevanos, and M. Orchard, "Machine condition prediction based on adaptive neuro-fuzzy and high-order particle filtering," *IEEE Trans. Ind. Electron.*, vol. 58, no. 9, pp. 4353–4364, Sep. 2011.

[32] B. Zhang, C. Sconyers, C. Byington, R. Patrick, M. Orchard, and G. Vachtsevanos, "A probabilistic fault detection approach: Application to bearing fault detection," *IEEE Trans. Ind. Electron.*, vol. 58, no. 5, pp. 2011–2018, May 2011.

[33] A. Saxena, J. Celaya, B. Saha, S. Saha, and K. Goebel, "Evaluating prognostics performance for algorithms incorporating uncertainty estimates," in *Proc. 2010 IEEE Aerospace Conf.*, Mar. 2010, pp. 1–11.

[34] L. Tang, M. Orchard, K. Goebel, and G. Vachtsevanos, "Novel metrics and methodologies for the verification and validation of prognostic algorithms," in *Proc. 2011 IEEE Aerospace Conf.*, Mar. 2011, pp. 1–8.

[35] W. He, N. Williard, C. Chen, and M. Pecht, "State of charge estimation for electric vehicle batteries using unscented Kalman filtering," *Microelectron. Rel.*, vol. 53, no. 6, pp. 840–847, Jun. 2013.

[36] M. Orchard, M. Cerda, B. Olivares, and J. Silva, "Sequential Monte Carlo methods for discharge time prognosis in lithium-ion batteries," *Int. J. Prognost. Health Manage.*, vol. 3, no. 10, pp. 1–12, 2012.

[37] M. Orchard, P. Hevia-Koch, B. Zhang, and L. Tang, "Risk measures for particle-filtering-based state-of-charge prognosis in lithium-ion batteries," *IEEE Trans. Ind. Electron.*, vol. 60, no. 11, pp. 5260–5269, Nov. 2013.

[38] United States Advanced Battery Consortium, Electric Vehicle Battery Test Procedures, Jan. 1996.

[39] T. A. a. L. Goodman, "Statistical inference about Markov chains," *Ann. Math. Statist.*, vol. 28, no. 1, pp. 89–110, 1957.

[40] L. Rabiner, "A tutorial on hidden Markov models and selected applications in speech recognition," *Proc. IEEE*, vol. 77, no. 2, pp. 257–286, Feb. 1989.

[41] J. S. Hunter, "The exponentially weighted moving average," *J. Qual. Technol.*, vol. 18, pp. 203–209, 1986.

[42] B. Olivares, M. Cerda, M. Orchard, and J. Silva, "Particle-filtering-based prognosis framework for energy storage devices with a statistical characterization of state-of-health regeneration phenomena," *IEEE Trans. Instrum. Meas.*, vol. 62, no. 2, Feb. 2013.

[43] M. Cerda, "Estimacion en linea del tiempo de descarga de baterias de ion-litio utilizando caracterizacion del perfil de utilizacion y metodos secuenciales de Monte Carlo," M.S. thesis, Univ. Chile, Santiago, Chile, 2012.

[44] M. Chen and G. Rincón-Mora, "Accurate electrical battery model capable of predicting runtime and I-V performance," *IEEE Trans. Energy Convers.*, vol. 21, no. 2, pp. 504–511, Jun. 2006.

Daniel A. Pola received his B.S. and M.Sc. degrees in electrical engineering from the University of Chile in 2012 and 2014, respectively.

His research interests include estimation and prognosis based on Bayesian algorithms, health management for energy storage devices, system identification, and control systems.

Hugo F. Navarrete received the B.Sc. degree in electrical engineering, and certification in civil electrical engineering from the University of Chile in 2013 and 2014, respectively.

His research interests include health management in energy storage devices, and automatic control.

Marcos E. Orchard (M'06) received the M.S., and Ph.D. degrees in Electrical and Computer Engineering from the Georgia Institute of Technology in 2005 and 2007, respectively.

He is Associate Professor at the Electrical Engineering Department, University of Chile. His current research interest is the design, implementation, and testing of real-time frameworks for fault diagnosis and failure prognosis, with applications to battery management systems, the mining industry, and finance.

Ricardo S. Rabié received the B.Sc. degree in electrical engineering, and certification in civil electrical engineering from the University of Chile in 2012 and 2013, respectively.

His research interests includes health management in energy storage devices and renewable energy.

Matías A. Cerda received the B.S. and M.Sc. degrees in electrical engineering from the Universidad de Chile, Santiago, in 2011 and 2012, respectively.

His research interests include prognostics and health management for energy storage devices based on optimal and suboptimal Bayesian algorithms.

Benjamín E. Olivares received the B.S. and M.Sc. degrees in electrical engineering from the Universidad de Chile, Santiago, in 2011 and 2012, respectively.

His research interests include prognostics and health management for energy storage devices based on optimal and suboptimal Bayesian algorithms.

Jorge F. Silva (S'06–M'09) received the Master of Science (2005) and Ph.D. (2008) in Electrical Engineering from the University of Southern California (USC).

He is Assistant Professor at the Electrical Engineering Department, University of Chile. His research interests include estimation and detection, statistical signal processing, information theory, and statistical learning.

Pablo A. Espinoza received the B.S. from Pontificia Universidad Católica de Chile in 2007, and an M.Sc. in Astronomy from the University of Arizona in 2012. He is currently pursuing an M.Sc. in Electrical Engineering at the Universidad de Chile.

His research interests include prognostics, optimization, and electric vehicle characterization.

Aramis Pérez received his B.Sc. degree (2002), and Licentiate degree (2005) in Electrical Engineering from the University of Costa Rica. He is an electrical engineering doctorate student at the University of Chile.

His research interests include parametric and non-parametric modeling, system identification, data analysis, machine learning, and manufacturing processes.